Toxicology in Vitro 37 (2016) 88–96

Contents lists available at ScienceDirect

Toxicology in Vitro

journal homepage: www.elsevier.com/locate/toxinvit

Separating chemotherapy-related developmental neurotoxicity from cytotoxicity in monolayer and neurosphere cultures of human fetal brain cells

Delyan P. Ivanov [a,*], Abdal-jabbar Al-Rubai [b], Anna M. Grabowska [a,1], Margaret K. Pratten [b,1]

[a] Cancer Biology, Division of Cancer and Stem Cells, School of Medicine, Queen's Medical Centre, University of Nottingham, Nottingham, UK
[b] School of Life Sciences, Queen's Medical Centre, University of Nottingham, Nottingham, UK

ARTICLE INFO

Article history:
Received 9 June 2016
Received in revised form 1 August 2016
Accepted 9 September 2016
Available online 10 September 2016

Keywords:
Neural stem cell
Preclinical screening model
In vitro neurotoxicity assay
Neuronal differentiation
Topoisomerase drugs
Repurposing chemotherapeutics

ABSTRACT

Chemotherapy-induced neurotoxicity can reduce the quality of life of patients by affecting their intelligence, senses and mobility. Ten percent of safety-related late-stage clinical failures are due to neurological side effects. Animal models are poor in predicting human neurotoxicity due to interspecies differences and most *in vitro* assays cannot distinguish neurotoxicity from general cytotoxicity for chemotherapeutics.

We developed *in vitro* assays capable of quantifying the paediatric neurotoxic potential for cytotoxic drugs. Mixed cultures of human fetal brain cells were differentiated in monolayers and as 3D-neurospheres in the presence of non-neurotoxic chemotherapeutics (etoposide, teniposide) or neurotoxicants (methylmercury). The cytotoxic potency towards dividing progenitors *versus* differentiated neurons and astrocytes was compared using: (1) immunohistochemistry staining and cell counts in monolayers; (2) through quantitative Western blots in neurospheres; and (3) neurosphere migration assays. Etoposide and teniposide, were 5–10 times less toxic to differentiated neurons compared to the mix of all cells in monolayer cultures. In contrast, the neurotoxicant methylmercury did not exhibit selectivity and killed all cells with the same potency. In 3D neurospheres, etoposide and teniposide were 24 to 10 times less active against neurons compared to all cells. These assays can be used prioritise drugs for local drug delivery to brain tumours.

1. Introduction

Neurotoxicity is a serious side-effect which can result in diminished cognitive, sensory and motor functions in patients. Neurotoxicity has grave implications for the patients' quality of life; it affects employability, family life and independence. More than 30% of drug safety failures in phase I and II clinical trials are due to neurologic side effects (Redfern et al., 2010; Cook et al., 2014). In addition 7%–10% of the discontinued drugs in late clinical trials and marketed drugs are withdrawn due to neurotoxicity (Guengerich, 2011; Siramshetty et al., 2016). These late-stage failures can be very expensive, affect thousands of patients and are among the top reasons for the increasing costs of bringing new medicines to market (Tsaioun et al., 2009).

While the neurotoxic side-effects of anti-cancer chemotherapy are often overlooked, they can have long-lasting impact on the quality of survivorship for patients. For example, adolescent patients treated with vincristine develop painful peripheral neuropathy that can last for years (Bukowinski et al., 2015) and accidental administration of the drug in the cerebrospinal fluid is fatal (Alcaraz et al., 2002). Peripheral neuropathy is a potentially dose-limiting side-effect of taxanes, platinates, bortezomib and thalidomide (Miltenburg & Boogerd, 2014). Although the blood-brain barrier protects the brain from most of the above chemotherapeutics, drugs which can distribute to the central nervous system decrease cognitive functions (*e.g.* 5-fluorouracil (Wefel et al., 2010)), precipitate encephalopathy (methotrexate (Shuper et al., 2000)), and damage the cerebellum (cytarabine (Lazarus et al., 1981)).

Neurotoxicity is even more important in the context of brain cancer, where drugs need to distribute to the central nervous system (CNS), either through the blood-brain barrier or *via* local delivery routes. Despite toxicities, some neurotoxic drugs are used in local intra-cerebrospinal fluid regimens to prevent and eliminate leptomeningeal metastases (Matloub et al., 2006; Chamberlain, 2012). Conroy et al. (2010) have reviewed the literature in order to identify chemotherapeutics with lower potential for neurotoxicity, which can be repurposed for local intra-cerebrospinal fluid therapy in children. The main problem they have identified is the lack of data for the neurotoxic effects for a large

* Corresponding author at: Cancer Biology, Division of Cancer and Stem Cells, Queen's Medical Centre, University of Nottingham, Nottingham NG7 2UH, UK.
E-mail addresses: delyan.ivanov@nottingham.ac.uk (D.P. Ivanov), mbxaa10@nottingham.ac.uk (A. Al-Rubai), anna.grabowska@nottingham.ac.uk (A.M. Grabowska), margaret.pratten@nottingham.ac.uk (M.K. Pratten).
[1] Joint senior authors.

http://dx.doi.org/10.1016/j.tiv.2016.09.007

number of anti-cancer drugs on the market. Therefore, repurposing drugs for local CNS therapy would require testing a large panel of cytotoxic drugs for their ability to cause neurological damage and contrasting that with the exposures necessary to eliminate tumours. In this respect, it is vital to develop methods to quickly identify and prioritise anticancer drugs without neurotoxic effects. The patient population most likely to benefit from local chemotherapy are children under three, in whom radiotherapy is contraindicated due to severe neurotoxicity.

The Organisation for Economic Co-operation and Development, the US Food and Drug Agency and the European Medicines Agency rely solely on *in vivo* data for neurotoxicity testing (OECD, 1997; OECD, 2007). However, animal models are poor in predicting neurotoxicity, and miss between 30 and 45% of drugs with known neurotoxic side effects (Olson et al., 2000). These rodent studies cost €300,000 per compound (Agarwal & Rice, 1997; Jenkinson, 2012; Knight & Rovida, 2014), use either 80 adult animals for neurotoxicity (OECD, 1997) or 80 litters (1000 pups) (OECD, 2007) for developmental neurotoxicity, and take from one month to a year to complete.

In contrast to animal studies, *in vitro* models for neurotoxicity testing offer higher throughput and the advantage of using human cells. Cell culture systems in 96- and 384-well plates allow for rapid testing of large sets of compounds at a range of doses. Although the cells are cultured in an artificial environment, using human tissue eliminates the risk of interspecies differences which plague animal studies (Leist & Hartung, 2013; Abbott et al., 1999; Singh & Ferrara, 2012). The increased throughput and the ability to correctly classify neurotoxic compounds have been demonstrated for a number of rodent tissue-based *in vitro* models (Zurich et al., 2013; Hayess et al., 2013). However, recent studies have shown important interspecies differences in chemical and drug neurotoxicity towards rodents and humans (Baumann et al., 2015). Therefore future *in vitro* models would need to be based on human tissue in order to model human toxicity and fully capitalise on the advantages of *in vitro* culture.

Detecting specific neurotoxic effects of cytotoxic drugs on the normal brain *in vitro* is challenging. The majority of cells in the brain are not dividing and are well-differentiated. In this respect, using dividing tumour (SH-SY5Y), myc-immortalised cell lines (LUHMES (Smirnova et al., 2015), ReNCell (Hoffrogge et al., 2006), iPSC (Schwartz et al., 2015)) or poorly differentiated progenitors (hESC, fetal brain (Ivanov et al., 2014; Ivanov et al., 2015)) could lead to many false-positive signals for cytotoxic drugs. While all chemotherapy drugs would appear neurotoxic for these cells, clinical data for drugs like topoisomerase II poisons (etoposide and teniposide), nitrosoureas (carmustine and lomustine), dactinomycin and temozolomide show no evidence of neurotoxicity (Conroy et al., 2010). Although LUHMES and SH-SY5Y cells can be differentiated to more mature phenotypes (Schildknecht et al., 2009), the presence of oncogenes makes them unsuitable to serve as normal controls in experiments comparing the response of tumour and normal cells.

Our recent work on human fetal brain neurospheres (Ivanov et al., 2014; Ivanov et al., 2015) showed that human neural progenitor cells are sensitive to etoposide and hypothesized that this is due to their relatively undifferentiated state. Similar results for the effects of chemotherapy on neural progenitors have been reported by Dietrich et al. (2006). While fetal brain cells are poorly suited to model adult neurotoxicity, they can be differentiated to mimic the developing brain of children under three, who will be most likely to receive local brain-targeted chemotherapy. In this manuscript we have differentiated human fetal brain progenitors by withdrawing mitogens in order to study the effects of chemotherapy on differentiated cultures. In addition we have contrasted the effects of topo II drugs (etoposide and teniposide) to that of the classic neurotoxicant methylmercury (Ekino et al., 2007; Counter & Buchanan, 2004; Castoldi et al., 2001).

We used three different experimental setups to distinguish between neurotoxicity and cytotoxicity (Fig. 1). The first set of experiments exposed a monolayer of differentiating neural stem cells to different concentrations of etoposide and teniposide for 6 days (Fig. 1A). At the end, Resazurin (Alamar blue) reduction was used as a surrogate measure for viability for some plates, while the cells in other plates were stained and counted for nuclei (DAPI positive), neurons (βIII-tubulin positive cells) and astrocytes (GFAP positive cells). The objective was to compare the general measures of cytotoxicity, such as metabolic cytotoxicity assays and total cell counts, to counting specific cell populations, such as neurons and astrocytes. Thus, general toxicity was distinguished from astrocyte or glia-specific toxicity.

The second experimental setup was based on methods validated by the European Centre for Validation of Alternative Methods (ECVAM) (Zurich et al., 2013), but used human fetal cells and three protein endpoints instead of rat cells and mRNA quantification. Levels of GAPDH were used as a surrogate marker for the viability of all cells in culture, while levels of βIII-tubulin and GFAP were used to quantify toxicity towards neurons and glia respectively. The human fetal brain cells were cultured with the drugs as neurospheres in uncoated plates for 6 days (Fig. 1B). Due to the three-dimensional nature of the cultures, we could not perform direct cell counts as in the previous setup, however there was sufficient amount of tissue to analyse protein levels by quantitative Western blot analysis.

The third experimental setup sought to explore the effect of topoisomerase inhibition on the migration potential of neural stem cells (Supplementary Fig. 1) (Moors et al., 2007). The cells were cultured as uniformly-sized neurospheres for 3 days, treated with the drugs for 24 h and then transferred into a coated plate to migrate for 48 h in the presence of each drug. Upon activation, neural stem cells in the normal brain need to be able to migrate from their niches to different regions of the brain in order differentiate, and maintain the steady state in the brain (Pilz et al., 2002; Sanai et al., 2011; Stiles & Jernigan, 2010). This experimental setup aimed to identify the levels of etoposide and teniposide which impair the natural migration potential of neural stem cells.

2. Materials and methods

2.1. Chemicals and reagents

Dulbecco's Modified Eagle Medium (DMEM), F12 Ham's Nutrient, Hank's balanced Salt Solution (HBSS), Phosphate Buffer Saline (PBS), Glutamine, Heparin, Accutase, poly-D-lysine (PDL), laminin, Resazurin, Brilliant blue dye, Triton X, bovine serum albumin (BSA), Dimethyl Sulfoxide (DMSO), and DAPI (4′,6-diamidino-2-phenylindole) were purchased from Sigma-Aldrich (UK). N2, B27 supplements, basic Fibroblast Growth Factor (bFGF) and Epidermal Growth Factor (EGF) were obtained from Invitrogen (Thermo Fisher Scientific, UK). Suspension cell culture flasks (non-treated, 25cm (Cook et al., 2014)) were supplied by PAA (GE Healthcare, Little Chalfont, UK), 48 well plates were obtained from Nunc (Thermo Fisher Scientific, UK), 96 well plates (Ultra Low attachment) were purchased from Corning (Flintshire, UK). The list of antibodies used in the experiments is given in Table 1.

2.2. Methods

2.2.1. Cell culture

Fetal human brain tissue was received from the Joint MRC/Wellcome Trust (grant # 099175/Z/12/Z, Ethics committee approval 08/H0906/21 + 5, Health Research authority NRES Committee North East - Newcastle & North Tyneside 1) Human Developmental Biology Resource (www.hdbr.org). The tissue was rinsed, mechanically dissociated into a single cell suspension and cultured in non-treated flasks to form stem cell enriched neurospheres (Uchida et al., 2000).

The Neural stem cell (NSC) defined serum-free media was made using DMEM/F12 (1:1), B27 (1:50), N2 (1:100), L-Glutamine (2 mM), human epidermal growth factor (EGF, 20 ng/ml), basic fibroblast

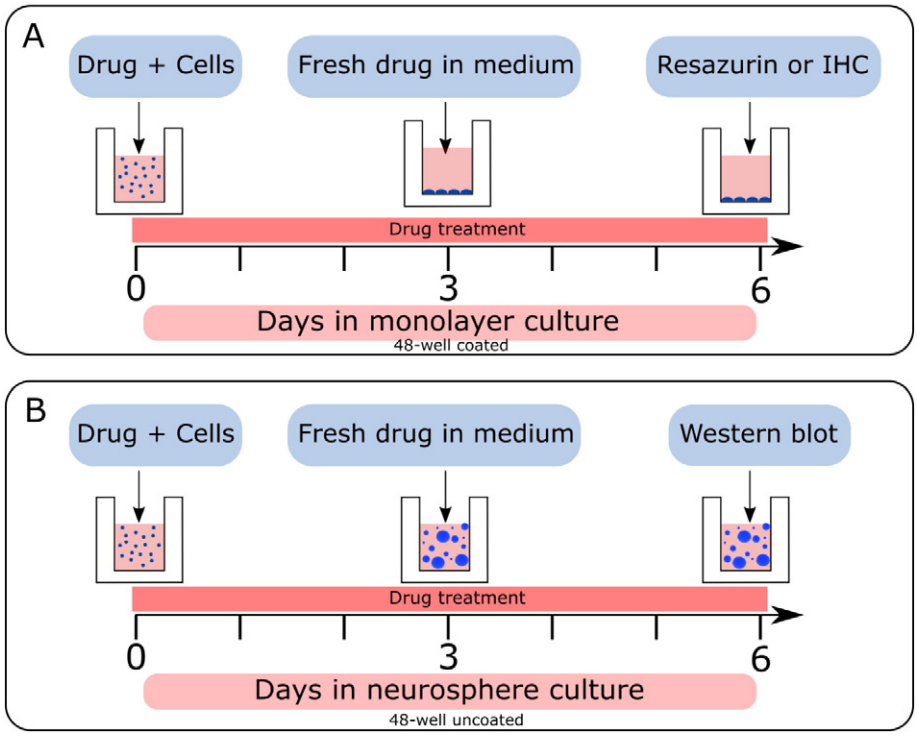

Fig. 1. Time course of the drug treatment protocols for monolayer (A), neurosphere (B) and migration (C) assays. A-human fetal brain cells were treated in differentiating conditions as monolayers with drug for 6 days in poly-D-lysine and laminin coated plates. Resazurin metabolism, number of nuclei (DAPI) and cells staining for βIII-tubulin or GFAP were used to compare general cytotoxic effects to lineage-specific toxicity. B-human fetal brain cells were cultured as neurospheres for 6 days and then the quantity of GAPDH, βIII-tubulin and GFAP quantified using Western blotting. GAPDH was used as a surrogate for all cells, βIII-tubulin for neurons, GFAP-astrocytes.

growth factor (FGF, 10 ng/ml) and Heparin (5 μg/ml). Neurospheres were subcultured for less than 25 passages as described by Ivanov et al. (2015). NSC Differentiation media composition was the same NSC media composition with the omission of EGF and FGF.

2.2.2. Differentiating monolayer cultures of fetal brain tissue

Differentiation of human fetal brain tissue-derived cells was performed in poly-D-lysine (PDL) and laminin coated 48-well plates. The plates were coated with PDL (5 μg/cm^2, overnight at room temperature), washed with distilled water (three times) and coated with laminin (2 μg/cm^2, 2 h at 37 °C).

Human fetal neurospheres were dissociated to form a single-cell suspension using Accutase (Ivanov et al., 2014) and were plated at 30,000 cells/well in NSC differentiation medium (500 μl) in 48-well plates.

Table 1
List of antibodies used in the Western blot and immunohistochemistry experiments.

Antibodies	Dilution	Sources	Cat. no
Western blot primary			
Mouse monoclonal anti-tubulin III antibody	1:2000	Abcam	ab78078
Rabbit polyclonal anti-GFAP antibody	1:20,000	Abcam	ab7260
Mouse monoclonal anti-GAPDH antibody	1:5000	Sigma	G8795
Western blot secondary			
Goat anti-mouse	1:30,000	Li-Cor Odyssey	926-32211
Goat anti-rabbit	1:30,000	Li-Cor Odyssey	926-68020
Immunohistochemistry primary			
Mouse monoclonal anti-tubulin III antibody	1:500	Abcam	ab7751
Rabbit polyclonal anti-GFAP antibody	1:800	Abcam	ab7260
Immunohistochemistry secondary			
Goat polyclonal anti-mouse IgG, Alexa Fluor 488	1:500	Abcam	ab150113
Goat polyclonal anti-rabbit IgG, Alexa Fluor 555	1:500	Abcam	ab150098

2.2.3. Drug treatment

All compounds were added immediately after seeding the cell suspension. Cells in untreated wells (controls) were suspended in 0.2% DMSO solution. Etoposide and teniposide were dispensed from separate stock solutions (500× in DMSO) for each concentration (final levels of 0.2% DMSO), in a set of six concentrations spaced in half-logarithmic steps. Methylmercury chloride was dissolved in distilled water. There were 6 technical replicates for each condition. The cells were incubated in the differentiation medium for 6 days and all media solutions were replaced every three days.

2.2.4. Resazurin metabolism-based viability assay

At the end of day 6, the medium was replaced with Resazurin solution (500 μl/well, 10 μg/ml, in HBSS), and the plate was left for 1 h at 37 °C in the incubator. Afterwards, fluorescence was measured with an excitation wavelength of 530 nm and emission 590 nm on a Galaxy Fluostar plate reader.

2.2.5. Immunohistochemistry

The same drug treatment concentrations as in Section 2.2.3 were used, with 2 technical replicates per condition. 20,000 cells were seeded in each well in differentiation media (500 μl), incubated for 6 days with one media change at day 3. At the end of day 6 the medium was aspirated and the cells were fixed in paraformaldehyde solution (4% wt/wt in PBS, 15 min). Combined blocking and permeabilization was done in Triton-X (0.25% vol/vol) and bovine serum albumin (1% wt/wt) for 30 min, followed by washing with PBS (three times, 5 min each). Primary antibodies anti-βIII-tubulin (1:500, TU-20 mouse monoclonal, Abcam ab7751) and anti-GFAP (1:800, rabbit polyclonal, Abcam ab7260) were added together overnight at 4 °C. On the next day, after washing with PBS (three times, 5 min each), secondary antibodies (goat polyclonal anti-mouse, Alexa Fluor 488 ab150113 and anti-rabbit IgG, Alexa Fluor 555 ab150098) were added in (1:500, 1 h). After a PBS

wash (3 times), nuclei were stained using 4′,6-diamidino-2-phenylindole - DAPI (1:1000, 2 min), followed by a final PBS wash (2 times). Wells were covered with glycerol mounting media (50:50 vol/vol glycerol:PBS) containing 2.5% wt/vol DABCO (1, 4-diazabicyclo-[2,2,2]-octane).

2.2.6. Fluorescence microscopy

Imaging was performed on a Nikon Ti Eclipse inverted fluorescence microscope using 4× objective for image quantification (Fig. 4) and images acquired at 20× for representative image illustrations (Fig. 3). Table 2 lists the filters used in the fluorescence microscopy experiments.

2.2.7. Image analysis algorithms

All images were analysed using the 2016 version Fiji Distribution (Schindelin et al., 2012) of ImageJ (Schindelin et al., 2015).

DAPI-stained nuclei images of all cells were thresholded using the Otsu algorithm (Otsu, 1979). Overlapping nuclei were separated using ImageJ's Watershed function and the number of particles with size between 10–1000 μm^2 counted for each condition.

The algorithm for quantifying βIII-tubulin cells included the following steps: manually set threshold to distinguish positive cells from background, noise removal filter (Despeckle), a minimum filter (radius = 2) to remove neuronal processes, watershed step to separate merging neuronal bodies and an "Analyze particles" final step to count cell-bodies, 30–2000 μm^2 in size, with circularity greater than 0.3.

Astrocytes were counted by applying a manually set threshold to hold to separate positive cells from background, noise removal filter (Despeckle), a minimum filter (radius = 2) and counting all particles with size from 50 to 10,000 μm^2.

2.2.8. Western blots

For the western blot experiments, 10,000 cells were seeded (NSC differentiation media, 500 μl) in uncoated 48 well plates with 6 technical replicates per condition. Drug treatment was done for 6 days with one medium change at day 3. On day 6, the media and the neurospheres were transferred to a microcentrifuge tube and centrifuged (13,000 RPM for 1 min). The supernatant was removed and the pellets were washed twice with ice cold PBS. Protein content was quantified and normalised using the Lowry assay and the western blot performed according to Qureshi (Shaikh Qureshi, 2012).

The primary antibodies were diluted in 5% milk solution and the dilutions were as follows: anti-tubulin III (mouse monoclonal antibody-Abcam ab78078) 1:2000, anti-GFAP (rabbit polyclonal antibody-Abcam ab7260) 1:20,000, anti-GAPDH (mouse monoclonal antibody-Sigma G8795) 1: 5000. Appropriate amounts of these antibodies were used in sealed nylon bags to incubate the blots overnight in the refrigerator at 4 °C on a plate shaker. On the next day, the blots were washed by TBST (50 mM Tris, 150 mM NaCl, 0.05% vol/vol Tween 20), three quick washes, three 5 min washes and three 15 min washes to remove non-specific binding. The secondary antibodies (IRDye 680LT goat anti-mouse IgG (H + L) and IRDye 800CW goat anti-rabbit IgG (H + L)) were used in 1:30,000 dilution in 5% milk solution in TBST. The blots were incubated with the secondary antibodies for 1 h on a plate shaker at room temperature and then washed with TBST. The blots were scanned using a Li-Cor Odyssey scanner and the intensity of the bands quantified with Image studio 3.0.

Table 2
Table of excitation and emission filters used in the fluorescence microscopy experiments.

Nikon filter (name, stained entity)	Excitation, nm	Emission, nm
DAPI, DNA, nuclei	358	461
GFP, βIII-tubulin (neurons)	488	507
tdTomato, GFAP (astrocytes)	554	581

2.2.9. Migration assay

The migration analysis was based on the technique described by Moors et al. (2007). Briefly, 10,000 cell per well were seeded in NSC media (100 μl) in ultra-low attachment plates, centrifuged (300 RCF, 3 min) and left in the incubator to form one centrally placed neurosphere per well. The neurospheres were cultured for 3 days until they reached 350–400 μm diameter. At day 3 the neurospheres were transferred to a 48 well plate (uncoated) and incubated for 24 h with NSC differentiation media, 500 μl/well. At this point etoposide and teniposide were added in a set of six concentrations spaced in half-log-arithmic steps as in Section 2.2.3.

After 24 h incubation with the drugs, the neurospheres and drug solutions were transferred to a 48-well plate coated with PDL and laminin (as described in Section 2.2.2). The neurospheres attached to the wells within a few hours and individual cells started migrating outwards. Photographs were taken at 0 h, 24 h and 48 h after plating for migration (24, 48 and 72 h with the drugs respectively). The migration distance was calculated as half of the difference between the diameter of the furthest migrating cells and the initial neurosphere diameter at t = 0 h. The diameter of the migrating cells was calculated as the mean of two perpendicular diameters of the furthest cells migrating outwards.

2.2.10. Data analysis

Raw data were exported and analysed in MS Excel and Graphpad Prism 6. Resazurin data were normalised relative to untreated control (100%) and cell-free wells (0%). Western blot, cell migration data and fluorescently labelled cell counts were normalised to untreated controls (100%) and 0 for (0%). Dose response curves were fitted using the four-parameter logistic equation in Prism, the top was constrained to 100% and the bottom to the viability at the highest drug concentration. IC50 used are the inflection point of the dose-response curve, half-way between the untreated controls (100%) and the curve bottom (maximum effect). Results are displayed as mean ± SD unless stated otherwise. The comparison of IC50 values was done using the logarithms of IC50 (logIC50) and the standard error of the IC50 from the non-linear regression analysis with the number of fitted points as n. The values for logIC50 for βIII-tubulin- and GFAP protein (Western blot experiments) or positive cells (immunohistochemistry experiments) were compared to the logIC50 for GAPDH or logIC50 for DAPI respectively using a one-way ANOVA with Dunnett's correction for multiple comparisons and the times differences between means plotted along with their 95%-confidence intervals (95%CIs).

3. Results

Both etoposide (Fig. 2A) and teniposide (Fig. 2B) elicited a dose-dependent decrease in cell viability in differentiating monolayer cultures of human fetal brain cells as measured by the Resazurin assay. While the metabolic activity of the cultures was reduced down to 30%, at the highest concentrations for both drugs, compared to untreated controls, the IC50 for teniposide was 4 times lower than etoposide.

In a separate experiment the differentiating fetal brain cells were treated with increasing concentrations of the neurotoxic methylmercury, etoposide and teniposide (Fig. 3). In order to distinguish the cell-lineage specific effects of the drugs all nuclei were stained with DAPI, neurons were stained for βIII-tubulin, while GFAP was used to identify astrocytes. In the untreated cultures βIII positive cells varied from 30 to 60%, while astrocytes were 10–40%. All tested compounds caused a dose-dependent decrease in the numbers of cells as a whole, the numbers of neurons and astrocytes. While, neurons were killed at higher concentrations compared to all cells in the etoposide and teniposide treated groups, mercury was equally toxic to all neural tissue cells (Fig. 3).

Dose-response curves for mercury, etoposide and teniposide were plotted when the numbers for all cells, neurons and astrocytes were quantified for each concentration and normalised to untreated controls.

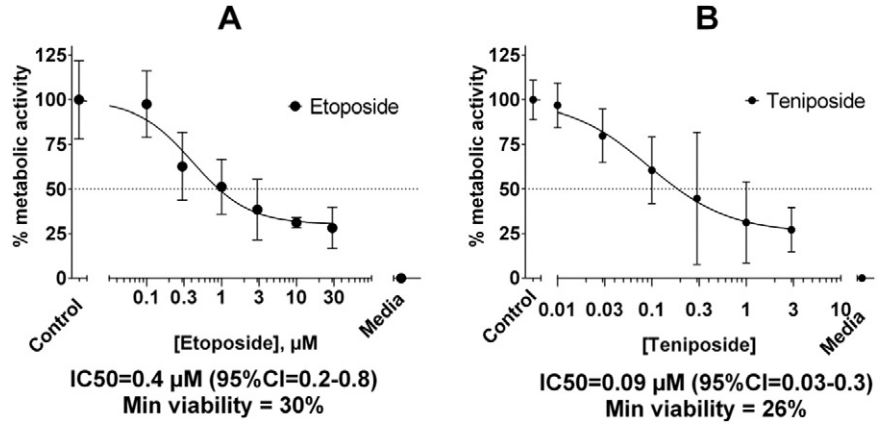

Fig. 2. Metabolic activity of differentiating neural progenitors, exposed to etoposide and teniposide. Resazurin reduction assay measured the metabolic activity of differentiating neural progenitors treated with increasing concentrations of etoposide (A) and teniposide (B) for 6 days. Metabolic activity is given as percentage compared to untreated control, error bars are standard deviations for 3 independent experiments.

All fetal brain cell populations appeared equally sensitive to mercury with IC50 in the nanomolar range. In contrast, the IC50s of βIII-tubulin expressing cells for etoposide and teniposide were 5 and 10 times higher respectively, when compared to the IC50s for all cells in the well (Fig. 4G). For both topoisomerase drugs, the difference in IC50s for βIII-tubulin-positive cells was statistically significant, while the difference for GFAP-positive ones was not (Fig. 4D and F).

In order to confirm the results from the monolayer experiments, the fetal brain cells were cultured in neurosphere conditions for 6 days in the presence of etoposide or teniposide (Fig. 1B). The amount of GAPDH, βIII-tubulin and GFAP were quantified by Western blot and used as surrogate measures for the number of all cells, neurons and astrocytes (Fig. 5A and C). Neurospheres were sensitive to etoposide and teniposide in the micromolar range, similarly to monolayers (Fig. 2). The levels of βIII-tubulin and GFAP proteins decreased at higher concentration compared to GAPDH for both drugs. The etoposide IC50s for βIII-tubulin and GFAP were 24 and 10 times higher than those for GAPDH and the differences were statistically significant using a one-way ANOVA test with Dunnett's correction for multiple comparisons (Fig. 5B and E). While the confidence intervals for teniposide IC50 values were quite variable, spanning almost an order of magnitude, the 9 times difference between βIII-tubulin and GAPDH was statistically significant (Fig. 5D and E).

Both etoposide (Supplementary Fig. 2A) and teniposide (Supplementary Fig. 2B) suppressed cell migration from fetal neurospheres in a dose-dependent manner. At the highest concentrations etoposide-treated neurospheres migrated to 27% of the distance compared to untreated controls (Supplementary Fig. 2C). Teniposide treated neurospheres migrated half the distance compared to controls. There was little difference in the relative decrease of cell migration when the

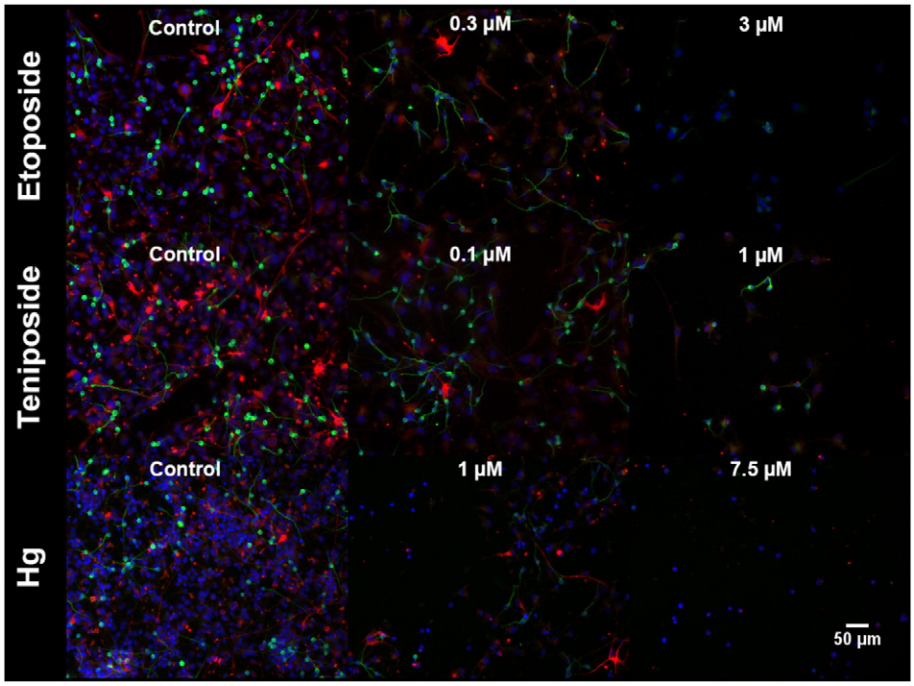

Fig. 3. Wide-field fluorescence images of fluorescently labelled human fetal brain cells cultured under differentiation conditions upon treatment with Etoposide (top), Teniposide (middle) and Mercury (Hg, bottom). Nuclei are coloured blue (DAPI), βiii-tubulin expressing cells are stained green and GFAP-positive cells are red. Left-hand images (untreated controls), middle section (intermediate concentrations, around IC50) and right-section (high concentrations).

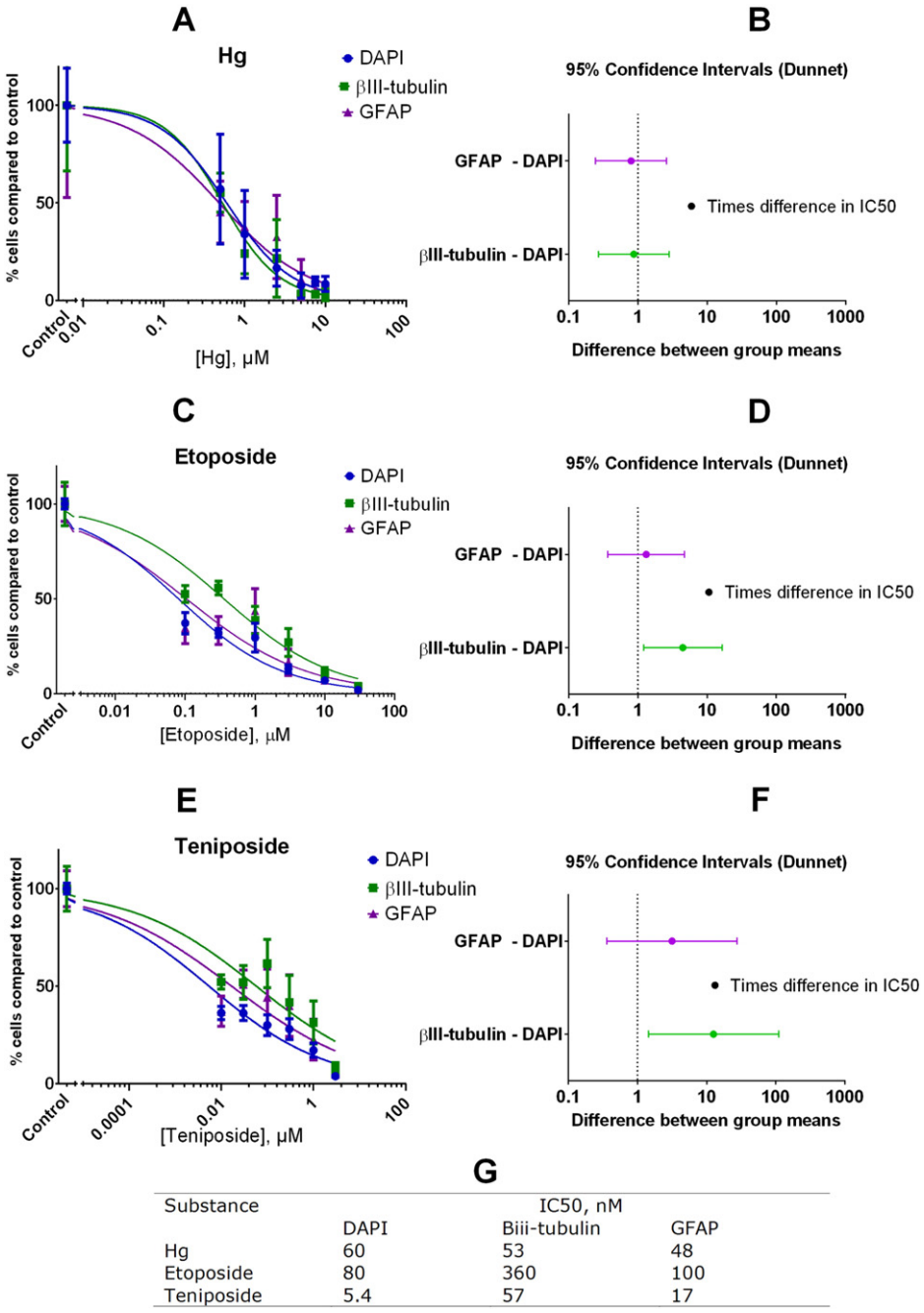

G

Substance	IC50, nM		
	DAPI	Biii-tubulin	GFAP
Hg	60	53	48
Etoposide	80	360	100
Teniposide	5.4	57	17

Fig. 4. Dose-response curves and comparison of IC50s for fluorescently-labelled cells. A,C,E - dose response curves for Hg, etoposide and teniposide respectively; The dose response curves for the number of nuclei of all cells are in blue, βiii-tubulin expressing cells (green) and GFAP-positive cells (purple). B,D,F differences between the logIC50s of βIII-tubulin expressing cells (green) and all nuclei (DAPI) and between GFAP-positive cells (purple) and all nuclei (DAPI), error bars represent the 95%-confidence intervals of the difference. G - table listing the IC50s for all dose response curves.

cells were left for 24 or 48 h. The effects seen on migration were seen at concentrations where both metabolism and cell viability would have been affected and therefore need to be interpreted with caution.

4. Discussion

Metabolism-based assay measuring reduction of substrates (MTT, MTS, Resazurin) or cellular ATP are widely utilised to measure cytotoxicity *in vitro* (Ivanov et al., 2014; Vinci et al., 2012). Although they are well-suited for homogenous monocultures, their utility for measuring viability in mixed populations and primary tissues may be limited. While these assays will reliably detect general cytotoxic effects, they may miss subtle differences in the sensitivity of different populations.

Etoposide and teniposide elicited a dose-dependent decrease in the metabolic activity (Fig. 2) and numbers of cells (Fig. 4) in differentiating monolayers of human fetal brain cells. However, the numbers of neurons and astrocytes dropped at higher concentrations compared to all cells in culture, which resulted in 5–10 fold higher IC50 values. This indicates that although etoposide and teniposide are cytotoxic, their neurotoxic potency is 5–10 times lower. In contrast to topoisomerase drugs, the neurotoxicant methylmercury was toxic to all cells regardless of differentiation status.

The immunohistochemistry results in 2D were supported by Western blot data in 3D human fetal brain neurospheres cultured for the same duration of time with etoposide and teniposide. There was good agreement between the IC50 values for metabolic activity in

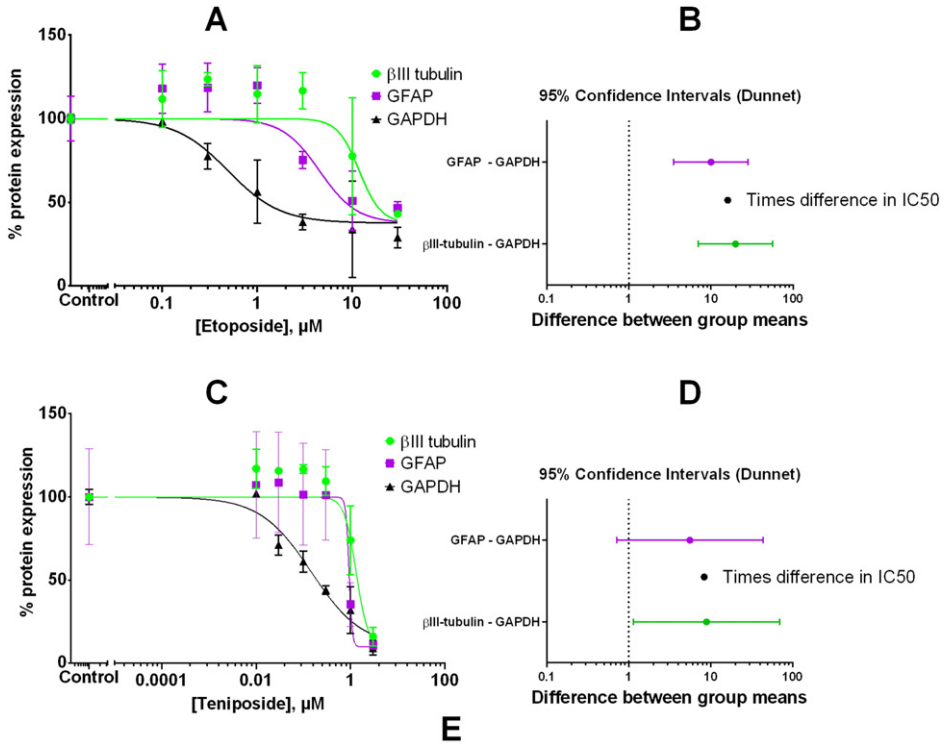

E

Protein	Etoposide		Teniposide	
	IC50 (95% CI) μM	Min quantity %	IC50 (95% CI) μM	Min quantity %
GAPDH	0.5 (0.2-1)	38	0.15 (0.034-0.6)	10
βIII-tubulin	12 (6-23)	38	1.3 (0.6-2.9)	10
GFAP	5 (2-9)	38	0.93 (very wide)	10

Fig. 5. Quantity of GAPDH, βIII-tubulin and GFAP proteins in human fetal neurospheres after 6-day treatment with etoposide and teniposide. A and C - dose-response curves for etoposide (A) and teniposide (C) GAPDH (black triangle), GFAP (purple square) and βIII-tubulin (green circle) for etoposide (A) and teniposide (C); Results from three independent experiments, error bars are standard deviations. B and D- times differences between the logIC50s for βIII-tubulin (green) and GAPDH and between GFAP-positive cells (purple) and GAPDH, error bars represent the 95%-confidence intervals of the times difference; E - summary table with IC50 values, confidence intervals and the minimal quantity of protein at the highest drug concentration compared to the untreated control.

monolayer cells and the IC50s derived from quantifying GAPDH in neurospheres. This is probably due to our setup of forming the neurospheres in the presence of drug and thus eliminating drug-neurosphere penetration issues. By using the quantity of GAPDH as a surrogate for all cells in the neurospheres, βIII-tubulin for the neurons and GFAP for the astrocytes we were able to detect differences in drug sensitivity between the cell-lineages. While the quantity of GAPDH quickly decreased at the lowest etoposide and teniposide concentrations, βIII-tubulin protein levels, dropped at 9–24 times higher levels. Similarly the IC50 for the astrocytic protein GFAP was 8 times higher compared to the IC50 for metabolic activity and GAPDH level. While these results may have been influenced by protein stability and turnover times, they are indicative of the resistance of differentiated cells to the effects of cytotoxic drugs.

These differences are not only statistically different, but they also have a practical clinical significance. The results show that etoposide and teniposide have a therapeutic window where they can be used in brain tumours without severely affecting the normal differentiated brain cells. The safe levels for etoposide were 0.3 μM (2D) to 3 μM (3D) for etoposide and 50 nM (2D) to 500 nM (3D) for teniposide respectively. In order to stand a chance in eliminating brain tumours at safe drug levels, the IC50s for etoposide and teniposide in tumour cells *in vitro* would need to be much lower than the concentrations above. The identified therapeutic window for etoposide, can explain the drug's lack of neurotoxic side effects when administered intrathecally in children at therapeutic concentrations (van der Gaast et al., 1992; Slavc et al., 2003; Fleischhack et al., 2001). It would also serve to explain data indicating neurotoxicity in animal studies using high doses of the drug (Savaraj et al., 1992).

Although neurons were less sensitive to etoposide in these experiments, they were still eliminated at the higher concentrations of etoposide. This highlights an important limitation of this study. Because βIII-tubulin is expressed in early neuronal progenitors, the observed effects are consistent with developmental neurotoxicity. However, the experimental setup does not answer the question whether topo II drugs would be equally toxic to the differentiated and mature nervous system of adults.

While βIII-tubulin expressing cells were shown to be more resistant to topoisomerase drugs, GFAP-expressing cells showed similar drug sensitivity to the overall mix of cells. Although GFAP is regarded as a marker for astrocytes, its δ-isoform is expressed in some populations of neural stem cells (Middeldorp & Hol, 2011) and GFAP-positive cells can divide more rapidly, compared to neurons. Therefore, selective cytotoxicity of topoisomerase poisons towards dividing cells may explain the effects on GFAP-positive cells. These data imply that etoposide and teniposide could exhibit toxicity towards dividing reactive astrocytes if administered locally after surgery. However the GFAP-positive cells in our experiments may be phenotypically different to the reactive astrocytes in the brains of brain tumour patients.

Interpreting the results of migration assays is often difficult for chemotherapy drugs affecting cell division and proliferation due to the synergism of suppressing proliferation and inhibiting migration. In our case, the dose-dependent decrease in migration occurred at doses sufficient to affect metabolism and cell viability indicating that the decrease

in migration distance may be due to the anti-proliferative effects of etoposide and teniposide. The shorter drug incubation period (3 days) *versus* (6 days) and adding the drugs after spheroid formation would also contribute to the decreased effect. Nevertheless, the data suggests that etoposide and teniposide do not inhibit migration at non-cytotoxic concentrations.

5. Conclusions

This work has shown that general cytotoxicity can be distinguished from developmental neurotoxicity in human fetal brain cultures by quantifying protein markers for neurons (βIII-tubulin) and astrocytes (GFAP). Quantification of differentiation markers on the protein level revealed 9–24 times increased resistance to topoisomerase drugs of the differentiated cells in fetal brain cultures compared to the mix of all cells. Moreover, while neurotoxic compounds, like mercury, killed all cells in fetal brain cultures, etoposide and teniposide were 5–10 times less toxic to cells of the neuronal lineage. The methodology can be used as a pre-screen to identify chemotherapy drugs with lower chance of causing neurological toxicity *in vitro*.

Direct cell kill of neuronal and glial cells is only one mechanism through which chemotherapy can cause neurotoxicity. More subtle changes such as **leukoencephalopathy** or disturbance in network function would need to be examined with other assay setups. Therefore this combination of methods cannot be used as a stand-alone substitute of animal experiments. It would be best suited as parf of a panel of assays which would also encompass functional endpoints such as myelination changes, and disturbance in electrical activity and network communication.

Supplementary data to this article can be found online at http://dx.doi.org/10.1016/j.tiv.2016.09.007.

Author contributions

DI, AJ, AG and MP conceived the experiments. AJ performed the experiments and collected the data, DI- acquired the fluorescence images, analysed the data from all experiments and drafted the article. DI, AJ, AG and MP authors revised the manuscript and produced the final version.

Transparency document

The Transparency document associated with this article can be found, in the online version.

Acknowledgements

Delyan Ivanov was supported by an EPSRC Doctoral Prize award hosted by the University of Nottingham (DP2014/DI). Abdal-jabbar Alrubai was sponsored by the Iraqi Ministry of Higher Education and Scientific Research (MOHESR-AA/11).

References

Abbott, B.D., et al., 1999. AhR, ARNT, and CYP1A1 mRNA quantitation in cultured human embryonic palates exposed to TCDD and comparison with mouse palate in vivo and in culture. Toxicol. Sci. 47, 62–75.

Agarwal, N., Rice, C., 1997. Additional information on small entity impacts of the amended proposed TSCA section 4(a) test rule for 21 hazardous air pollutants. https://yosemite1.epa.gov/ee/epa/ria.nsf/vwAN/TS0000365E-03.pdf/$file/TS0000365E-03.pdf.

Alcaraz, A., Rey, C., Concha, A., Medina, A., 2002. Intrathecal vincristine: fatal myeloencephalopathy despite cerebrospinal fluid perfusion. J. Toxicol. Clin. Toxicol. 40, 557–561.

Baumann, J., et al., 2015. Comparative human and rat neurospheres reveal species differences in chemical effects on neurodevelopmental key events. Arch. Toxicol. http://dx.doi.org/10.1007/s00204-015-1568-8.

Bukowinski, A.J., Burns, K.C., Parsons, K., Perentesis, J.P., O'Brien, M.M., 2015. Toxicity of cancer therapy in adolescents and young adults (AYAs). Semin. Oncol. Nurs. 31, 216–226.

Castoldi, A.F., Coccini, T., Ceccatelli, S., Manzo, L., 2001. Neurotoxicity and molecular effects of methylmercury. Brain Res. Bull. 55, 197–203.

Chamberlain, M.C., 2012. Neurotoxicity of intra-CSF liposomal cytarabine (DepoCyt) administered for the treatment of leptomeningeal metastases: a retrospective case series. J. Neuro-Oncol. 109, 143–148.

Conroy, S., et al., 2010. Medulloblastoma in childhood: revisiting intrathecal therapy in infants and children. Cancer Chemother. Pharmacol. 65, 1173–1189.

Cook, D., et al., 2014. Lessons learned from the fate of AstraZeneca's drug pipeline: a five-dimensional framework. Nat. Rev. Drug Discov. 13, 419–431.

Counter, S.A., Buchanan, L.H., 2004. Mercury exposure in children: a review. Toxicol. Appl. Pharmacol. 198, 209–230.

Dietrich, J., Han, R., Yang, Y., Mayer-Pröschel, M., Noble, M., 2006. CNS progenitor cells and oligodendrocytes are targets of chemotherapeutic agents in vitro and in vivo. J. Biol. 5, 22.

Ekino, S., Susa, M., Ninomiya, T., Imamura, K., Kitamura, T., 2007. Minamata disease revisited: an update on the acute and chronic manifestations of methyl mercury poisoning. J. Neurol. Sci. 262, 131–144.

Fleischhack, G., et al., 2001. Feasibility of intraventricular administration of etoposide in patients with metastatic brain tumours. Br. J. Cancer 84, 1453–1459.

Guengerich, F.P., 2011. Mechanisms of drug toxicity and relevance to pharmaceutical development. Drug Metab. Pharmacokinet. 26, 3–14.

Hayess, K., et al., 2013. The DNT-EST: a predictive embryonic stem cell-based assay for developmental neurotoxicity testing in vitro. Toxicology 314, 135–147.

Hoffrogge, R., et al., 2006. 2-DE proteome analysis of a proliferating and differentiating human neuronal stem cell line (ReNcell VM). Proteomics 6, 1833–1847.

Ivanov, D.P., et al., 2014. Multiplexing spheroid volume, resazurin and acid phosphatase viability assays for high-throughput screening of tumour spheroids and stem cell neurospheres. PLoS One 9, e103817.

Ivanov, D.P., et al., 2015. In vitro co-culture model of medulloblastoma and human neural stem cells for drug delivery assessment. J. Biotechnol. http://dx.doi.org/10.1016/j.jbiotec.2015.01.002.

Jenkinson, P., 2012. Survey of worldwide CROs: costs and practicalities of two new OECD guidelines for testing chemical substances: OECD 443, extended one-generation reproductive toxicity study, and OECD 488, transgenic rodent somatic and germ cell mutation assay. https://echa.europa.eu/documents/10162/13628/survey_report_worldwide_cros_en.pdf.

Knight, J., Rovida, C., 2014. Safety evaluations under the proposed US Safe Cosmetics and Personal Care Products Act of 2013: animal use and cost estimates. ALTEX http://dx.doi.org/10.14573/altex.1309271.

Lazarus, H.M., et al., 1981. Central nervous system toxicity of high-dose systemic cytosine arabinoside. Cancer 48, 2577–2582.

Leist, M., Hartung, T., 2013. Inflammatory findings on species extrapolations: humans are definitely no 70-kg mice1. ALTEX 30, 227–230.

Matloub, Y., et al., 2006. Intrathecal triple therapy decreases central nervous system relapse but fails to improve event-free survival when compared with intrathecal methotrexate: results of the Children's Cancer Group (CCG) 1952 study for standard-risk acute lymphoblastic leukemi. Blood 108, 1165–1173.

Middeldorp, J., Hol, E.M., 2011. GFAP in health and disease. Prog. Neurobiol. 93, 421–443.

Miltenburg, N.C., Boogerd, W., 2014. Chemotherapy-induced neuropathy: a comprehensive survey. Cancer Treat. Rev. 40, 872–882.

Moors, M., Cline, J.E., Abel, J., Fritsche, E., 2007. ERK-dependent and -independent pathways trigger human neural progenitor cell migration. Toxicol. Appl. Pharmacol. 221, 57–67.

OECD, 1997. OECD Guidelines for the Testing of Chemicals Section 4. OECD Publishing http://dx.doi.org/10.1787/9789264071025-en.

OECD, 2007. OECD Guidelines for the Testing of Chemicals Section 4. OECD Publishing http://dx.doi.org/10.1787/9789264067394-en.

Olson, H., et al., 2000. Concordance of the toxicity of pharmaceuticals in humans and in animals. Regul. Toxicol. Pharmacol. 32, 56–67.

Otsu, N., 1979. A threshold selection method from gray-level histograms. IEEE Trans. Syst. Man Cybern. 9, 62–66.

Pilz, D., Stoodley, N., Golden, J.A., 2002. Neuronal migration, cerebral cortical development, and cerebral cortical anomalies. J. Neuropathol. Exp. Neurol. 61, 1–11.

Redfern, W.S., et al., 2010. Impact and frequency of different toxicities throughout the pharmaceutical life cycle. Toxicology 114, 1081.

Sanai, N., et al., 2011. Corridors of migrating neurons in the human brain and their decline during infancy. Nature 478, 382–386.

Savaraj, N., et al., 1992. Pharmacology of intrathecal VP-16-213 in dogs. J. Neuro-Oncol. 13, 211–215.

Schildknecht, S., et al., 2009. Requirement of a dopaminergic neuronal phenotype for toxicity of low concentrations of 1-methyl-4-phenylpyridinium to human cells. Toxicol. Appl. Pharmacol. 241, 23–35.

Schindelin, J., et al., 2012. Fiji: an open-source platform for biological-image analysis. Nat. Methods 9, 676–682.

Schindelin, J., Rueden, C.T., Hiner, M.C., Eliceiri, K.W., 2015. The ImageJ ecosystem: an open platform for biomedical image analysis. Mol. Reprod. Dev. 82, 518–529.

Schwartz, M.P., et al., 2015. Human pluripotent stem cell-derived neural constructs for predicting neural toxicity. Proc. Natl. Acad. Sci. U. S. A. 112, 12516–12521.

Shaikh Qureshi, W.M., 2012. The chick cardiomyocyte micromass system and stem cell differentiation along specific pathways: prediction of embryotoxic effects and their mechanism. http://eprints.nottingham.ac.uk/12773/.

Shuper, A., et al., 2000. Methotrexate treatment protocols and the central nervous system: significant cure with significant neurotoxicity. J. Child Neurol. 15, 573–580.

Singh, M., Ferrara, N., 2012. Modeling and predicting clinical efficacy for drugs targeting the tumor milieu. Nat. Biotechnol. 30, 648–657.

Siramshetty, V.B., et al., 2016. WITHDRAWN—a resource for withdrawn and discontinued drugs. Nucleic Acids Res. 44, D1080–D1086.

Slavc, I., et al., 2003. Feasibility of long-term intraventricular therapy with mafosfamide (n = 26) and etoposide (n = 11): experience in 26 children with disseminated malignant brain tumors. J. Neuro-Oncol. 64, 239–247.

Smirnova, L., et al., 2015. A LUHMES 3D dopaminergic neuronal model for neurotoxicity testing allowing long-term exposure and cellular resilience analysis. Arch. Toxicol. 1–19 http://dx.doi.org/10.1007/s00204-015-1637-z.

Stiles, J., Jernigan, T.L., 2010. The basics of brain development. Neuropsychol. Rev. 20, 327–348.

Tsaioun, K., Bottlaender, M., Mabondzo, A., 2009. ADDME–Avoiding Drug Development Mistakes Early: central nervous system drug discovery perspective. BMC Neurol. 9 (Suppl. 1), S1.

Uchida, N., et al., 2000. Direct isolation of human central nervous system stem cells. Proc. Natl. Acad. Sci. 97, 14720–14725.

van der Gaast, A., Sonneveld, P., Mans, D.R., Splinter, T.A., 1992. Intrathecal administration of etoposide in the treatment of malignant meningitis: feasibility and pharmacokinetic data. Cancer Chemother. Pharmacol. 29, 335–337.

Vinci, M., et al., 2012. Advances in establishment and analysis of three-dimensional tumor spheroid-based functional assays for target validation and drug evaluation. BMC Biol. 10, 1–21.

Wefel, J.S., Saleeba, A.K., Buzdar, A.U., Meyers, C.A., 2010. Acute and late onset cognitive dysfunction associated with chemotherapy in women with breast cancer. Cancer 116, 3348–3356.

Zurich, M.G., Stanzel, S., Kopp-Schneider, A., Prieto, P., Honegger, P., 2013. Evaluation of aggregating brain cell cultures for the detection of acute organ-specific toxicity. Toxicol. in Vitro 27, 1416–1424.